

# Advanced RANS modeling of wingtip vortex flows

By A. Revell<sup>†</sup>, G. Iaccarino AND X. Wu

The numerical calculation of the trailing vortex shed from the wingtip of an aircraft has attracted significant attention in recent years. An accurate prediction of the flow over the wing is required to provide the correct initial conditions for the trailing vortex, while careful modeling is also necessary in order to account for the turbulence in the vortex core. As such, recent works have concluded that in order to achieve results of satisfactory accuracy, the use of complex turbulence modeling closures and numerical grids of considerable size is an absolute necessity. In Craft *et al.* (2006) it was proposed that a Reynolds stress-transport model (RSM) should be used, while Duraisamy & Iaccarino (2005) obtained optimal results with a version of the  $v^2 - f$  which was specifically sensitised to streamline curvature. The authors report grid requirements upward of  $7 \times 10^6$  grid points, highlighting the substantial numerical cost involved with predicting this flow.

The computations here are reported for the flow over a NACA0012 half-wing with rounded wingtip at an incidence angle of  $10^\circ$ , as measured by Chow *et al.* (1997). The primary aim is to assess the performance of a new turbulence modeling scheme which accounts for the stress-strain misalignment effects in a turbulent flow. This three-equation model bridges the gap between popular two equation eddy-viscosity models (EVM) and the seven equations of a RSM. Relative to a RSM, this new approach inherits the stability advantages of an eddy-viscosity scheme, together with a lower computational expense, and it has already been validated for a range of unsteady mean flows (Revell 2006).

---

## 1. Introduction

The wingtip vortex flow is a case of particular relevance for aviation regulations such as landing and takeoff separation distances between aircraft. The characteristic swirling trailing vortices are known to be particularly hazardous to a lighter following aircraft, and while strict guidelines are in place to specify safe distances, the satisfactory prediction of these flows continues to challenge CFD techniques.

The study of trailing vortices is also pertinent to the development of novel wingtip devices, or so called 'wingtip sails', which can deliver an improved aerodynamic performance to the wing. An accurate design assessment could potentially be crucial within the fine economic margins of the commercial aircraft industry. These phenomena are also directly relevant to the flow around consecutive blades on a helicopter rotor, where the complex interaction of these vortices is a major source of noise and vibration.

The complex nature of the near-field region of a tip vortex is a combination of strongly turbulent three-dimensional effects, multiple separations and vortex interactions. Streamwise vorticity separates from the wing surface and rolls up into the primary tip vortex, which subsequently combines with secondary and tertiary structures, thus shifting the path of the vortex core upwards and inboard (Thompson 1983). Early analytical work by Batchelor (1964) showed that the axial velocity at the vortex core should increase above the freestream value as a result of radial equilibrium requirements, which was first

<sup>†</sup> MACE, University of Manchester, UK

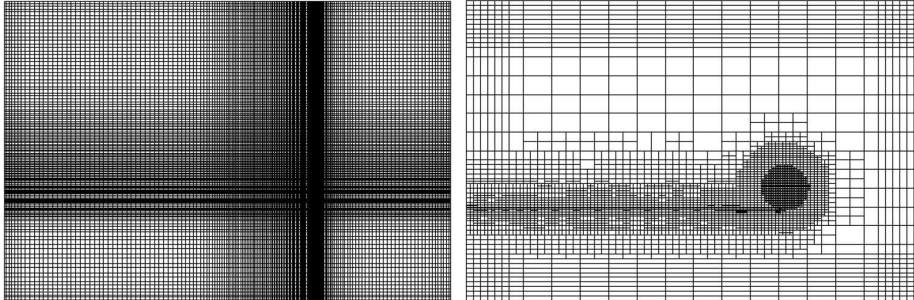


FIGURE 1. A comparison of the spanwise numerical mesh taken just downstream of the trailing edge from (*left*) a structured mesh of  $7.3 \times 10^6$  cells; and (*right*) an unstructured mesh of  $0.75 \times 10^6$  cells; a factor of 10 less.

observed experimentally by Orloff (1974). The experimental studies report a large reduction of turbulence levels within the vortex core, implying that the turbulent diffusion is small. Over-prediction of the turbulent diffusion in CFD can dramatically increase the predicted decay rate of the vortex, and thus its estimated downstream influence (Zeman 1995).

The primary aim of this study is to validate the stress-strain lag misalignment model for essentially steady flows with strong streamline-curvature. Secondary to this objective is to test an advanced unstructured meshing tool, which has the potential to offer huge economies in grid meshing (see figure 1). Both these goals serve a greater common purpose, which is the delivery of practical and economic alternatives to industrial users, where time and cost constraints are paramount.

## 2. Turbulence modeling of trailing vortices

The high Reynolds numbers typical of these flows render the cost of Large Eddy Simulation (LES) prohibitive and has tended to encourage the use of the more simple, more stable Reynolds Averaged Navier Stokes (RANS) models. However the experimental data of swirling flows has shown that these phenomena cannot be captured correctly at this level. The trailing vortex is an example of a flow with strong streamline curvature, a feature that is known to be inadequately represented by a linear EVM. Early attempts to correct this weakness focused upon the empirical length-scale-determining equation, but more recently it has become accepted that it is the stress-strain rate connection itself which requires attention.

The selected turbulence model must be capable of resolving the complex wing boundary layer as well as the swirling free shear flow downstream and as such it is perhaps unsurprising that relatively few CFD studies of this case have been reported. An early attempt by De Jong *et al.* (1988) at computing the vortex wake employing a simplified time-marching approach showed limited success. The first fully 3D fully-elliptic study was made by Dacles-Mariani *et al.* (1995), who used a structured grid of  $1.5 \times 10^6$  nodes and selected the basic model of Baldwin & Barth (1990). In this more recent work the authors highlighted the need to modify the turbulence model to prevent excessive diffusion, which essentially corresponds to a curvature correction.

In a European Union collaborative research project involving this testcase, it was seen

that of a large selection of turbulence models, only the Reynolds stress models were consistently able to reproduce the correct axial-velocity overshoot (Haase *et al.* 2006). While the linear EVMs greatly overpredicted the decay rate of the vortex, several other eddy viscosity schemes with ‘curvature-sensitive’ terms performed reasonably well; the  $LLR - k - \omega$  model of Rung & Thiele (1996) and the CEASM of Lübcke *et al.* (2002) are two such models. A range of numerical grids were used ( $4.2 \times 10^6 - 7.3 \times 10^6$  cells), and a strong grid sensitivity was clearly observed. The most accurate results were found when the largest grid was combined with the non-linear Reynolds stress-transport model of Craft *et al.* (1996a), the results of which are reported in the more detailed study of Craft *et al.* (2006).

The work by Duraisamy & Iaccarino (2005) on this case proposed a curvature correction for the original  $v^2 - f$  model of Durbin (1991), whereby the eddy-viscosity coefficient,  $C_\mu$ , was replaced by an algebraic expression sensitive to invariants of strain and vorticity. The authors reported that the characteristic axial-velocity overshoot above the freestream value was picked up only when the correction was applied, and a good agreement with mean velocity and turbulent quantities were observed. In this work the authors used a numerical grid containing approximately  $9.3 \times 10^6$  cells.

The increase in computational power over the last decade is reflected in the trend towards larger numerical grids, with the recent work by Duraisamy & Iaccarino (2005) reporting grid-independent solutions. The most recent work on this case is an LES study by Uzun *et al.* (2006) who computed the flow at the lower Reynolds number of  $0.5 \times 10^6$  in order to reduce the computational cost to an acceptable level. Despite this measure, a numerical grid of  $26.2 \times 10^6$  nodes was required, and the authors report using 124 processors for between 23 – 57 days dependent upon the processor speed. In addition, the reduction of Reynolds number is seen to have a considerable effect on the predicted results. While the scale of this work is impressive it serves to underline the substantial costs associated with using LES for flows of this nature.

### 3. The $C_{as}$ model

#### 3.1. Background

The present work seeks to validate a new turbulence modeling approach, originally developed for unsteady mean flows (Revell *et al.* 2006). The new approach builds upon existing two equation models with a third transport equation that is sensitive to the local stress-strain misalignment of mean unsteady turbulent flow. The new model considers a parameter,  $C_{as}$ , representing the dot product of the strain tensor  $S_{ij}$ , and the stress anisotropy tensor  $a_{ij}$  as follows:

$$C_{as} = -\frac{a_{ij}S_{ij}}{\sqrt{2S_{ij}S_{ij}}}, \quad S_{ij} = \frac{1}{2} \left( \frac{\partial U_i}{\partial x_j} + \frac{\partial U_j}{\partial x_i} \right), \quad a_{ij} = \frac{\overline{u_i u_j}}{k} - \frac{2}{3} \delta_{ij} \quad (3.1)$$

where  $U_j$  is the mean velocity vector,  $\overline{u_i u_j}$  is the Reynolds stress tensor,  $k$ , is the turbulent kinetic energy and  $\delta_{ij}$  is the Kronecker delta. The quantity  $C_{as}$  projects the six equations of the Reynolds stress transport onto a single equation. With respect to Non-Linear Eddy Viscosity Models (NLEVM) or Explicit Algebraic Reynolds Stress Models (EARSMS), the novelty of the present model lies in incorporating time dependent and/or transport effects of the turbulent stresses.

Both the stress anisotropy and strain rate are  $3 \times 3$  symmetrical tensors, and the associated eigenvectors are therefore real and orthogonal. The anisotropy tensor has zero

---

$\alpha_1$	$\alpha_1^*$	$\alpha_3$	$\alpha_3^*$	$\alpha_4$	$\alpha_5$	$\sigma_{cas}$
-0.70	-1.90	0.267	0.1625	0.75	1.60	0.2

TABLE 1. Coefficients of the  $C_{as}$  equation

trace and is dimensionless by definition, whereas the strain rate tensor is an inverse time scale and has zero trace only in the condition of incompressibility, which is assumed for this work. As previously stated, an EVM assumes that these two tensors are aligned.

The alignment for all quasi-2D flows is representable by a single dimensionless scalar. Three scalar values are necessary to define the stress-strain misalignment in a fully 3D flow, but in such cases, it is argued that at least some benefit will be gained from the scalar measure described above. Analysis of the tensorial alignment between the strain rate tensor  $S_{ij}$  and the turbulent stress anisotropy tensor  $-a_{ij}$  has been used extensively to gain an insight into complex energy transfer mechanisms (A minus sign is associated with  $a_{ij}$  to provide a direct assessment of the influence of alignment upon production of turbulent kinetic energy.), and also in the development of subgrid-scale stress models in LES (eg. see Bergstrom & Wang 2005).

An early attempt to account for the stress-strain misalignment was proposed by Rotta (1979), who proposed a simplified tensorial eddy viscosity formulation to account for these effects in 3D thin-shear boundary layer flows. Although it does not directly deal with the issue of misalignment, the more recent lag model of Olsen & Coakley (2001) couples a baseline two equation model with a third transport equation for the eddy viscosity,  $\nu_t$ . This modification enables relaxation effects to be captured and therefore prevents the eddy viscosity from responding instantaneously to changes in the mean strain rate field, and some improvements over the baseline two equation model are observed for non-equilibrium flows.

### 3.2. Implementation

The strategy adopted within the present work is to develop a transport equation that could be solved to obtain values for the parameter  $C_{as}$ . The resulting values could then be used in the evaluation of production of turbulence kinetic energy  $P_k$ , within an EVM framework, in order to capture some of the features of stress-strain misalignment, but at a much smaller computational cost than employing a full stress transport model. For details on the derivation see Revell (2006). The final implemented form of the transport equation is given as follows:

$$\begin{aligned}
 \frac{DC_{as}}{Dt} = & \underbrace{\alpha_1 \frac{\varepsilon}{k} C_{as}}_1 + \underbrace{\alpha_1^* \|S\| C_{as}^2}_2 + \underbrace{(\alpha_3 + \alpha_3^* \sqrt{a_{ij} a_{ij}}) \|S\|}_3 + \underbrace{\alpha_4 \frac{S_{ij} a_{ik} S_{jk}}{\|S\|}}_4 \\
 & + \underbrace{\alpha_5 \frac{S_{ij} a_{ik} \Omega_{jk}}{\|S\|}}_5 - \underbrace{\frac{1}{\|S\|} \frac{DS_{ij}}{Dt} \left( a_{ij} + \frac{2S_{ij} C_{as}}{\|S\|} \right)}_6 + \frac{\partial}{\partial x_k} \left[ (\nu + \sigma_{cas} \nu_t) \frac{\partial C_{as}}{\partial x_k} \right]
 \end{aligned} \tag{3.2}$$

where  $\varepsilon$  is the rate of dissipation of  $k$ , the strain invariant  $\|S\| = \sqrt{2S_{ij}S_{ij}}$ , the vorticity tensor  $\Omega_{ij} = 1/2(\partial U_i/\partial x_j - \partial U_j/\partial x_i)$ , the strain rate parameter  $\eta = k \|S\| / \varepsilon$  and the

model constants are given in Table 1. Since 3.2 is derived directly from an RSM, the constants of the selected pressure-strain model are retained and so in general, there is no requirement to calibrate these constants. It should be noted that when 3.2 is coupled with the baseline  $k - \omega$  SST model, it becomes necessary to use  $\varepsilon = 0.09k\omega$  in order to obtain a value for  $\varepsilon$  in Term 1.

The advection of the rate of strains in Term 6 of 3.2 is calculated explicitly as follows, where the superscript  $n$  refers to the calculation timestep, the size of which is denoted as  $\Delta t$ :

$$\frac{DS_{ij}}{Dt} = \frac{S_{ij}^n - S_{ij}^{n-1}}{\Delta t} + U_k \frac{\partial S_{ij}^n}{\partial x_k} \quad (3.3)$$

Equation 3.2 is not in closed form as a model for  $a_{ij}$  is still required. This can be obtained from any existing NLEVM, and in the present work the model of Craft *et al.* (1996b) has been selected for this purpose.

The current version of the  $C_{as}$  model requires special treatment in the near-wall region as a consequence of the modeling of the pressure-strain terms which are used in the derivation of 3.2. For high Reynolds number flows of the kind considered in the present work, the simplest treatment consists of preventing the model from acting in regions where viscous effects are expected to be dominant.

#### 4. Numerical setup

In this work the calculations were performed using the *in-house* CFD code, *Code\_Saturne* from EDF (Archambeau 2004). This is an unstructured finite-volume code based on a collocated discretization for cells of any shape. It solves turbulent Navier-Stokes equations for Newtonian incompressible flows with a fractional step method based on a prediction-correction algorithm for pressure/velocity coupling (SIMPLEC) and a momentum interpolation to avoid pressure oscillations. A number of turbulence models are available including the Shear Stress Transport (SST) of Menter (1994) and the Reynolds stress transport model of Speziale *et al.* (1991) (SSG) which are used in this work. The current form of the transport equation for  $C_{as}$  described in the previous section has been fully implemented into *Code\_Saturne*.

The fully implemented SST model requires only small modifications to incorporate the  $C_{as}$  model. Initially, the modification was intended to be applied to the production rate of turbulence kinetic energy term only, but it can be applied in a more coherent manner by means of a simple modification to the turbulent eddy viscosity as follows:

$$\nu_t = k \min \left( \frac{1}{\omega}; \frac{0.31}{\|S\| F_2}; \frac{C_{as}}{\|S\|} \right) \quad (4.1)$$

where  $\omega$  is the turbulent frequency and  $F_2$  is a blending function which takes a value  $\approx 1$  across most of the boundary layer, dropping to 0 near the top and in the free-stream (see Menter 1994 for details). The value of  $C_{as}$  in 4.1 is limited to  $\pm 0.31$  for the calculation of the production terms, while when evaluating diffusion terms, the absolute value,  $|C_{as}|$ , is used to avoid negative values which could lead to numerical difficulties.

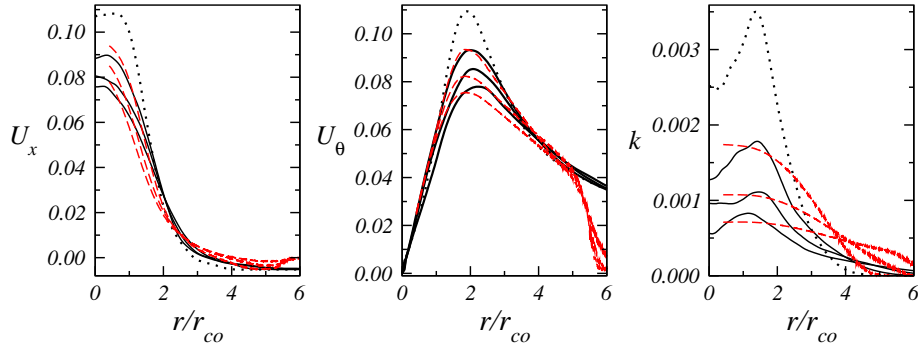
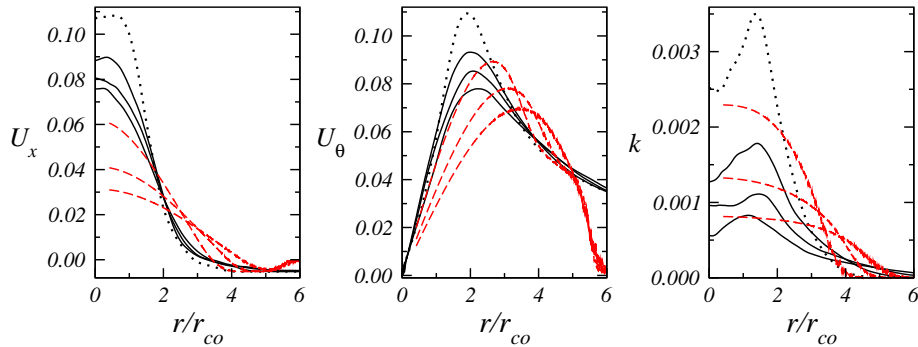
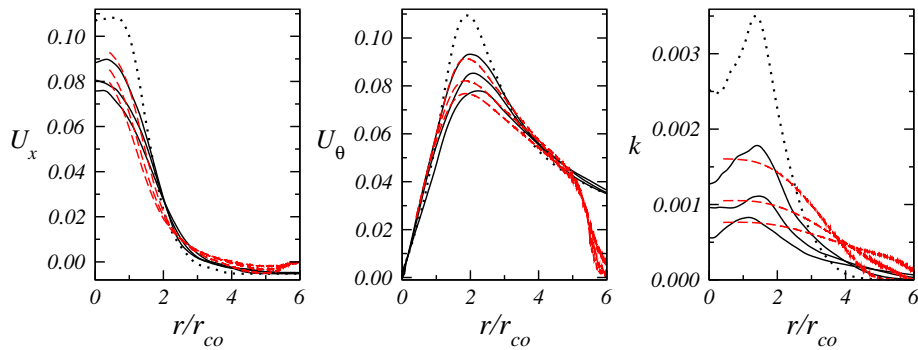
**a) RSM (SSG)****b) SST****c) SST -  $C_{as}$** 

FIGURE 2. Evolution of mean velocity and turbulent kinetic energy. RANS calculations initialized from DNS values at  $t/T = 2.0$  (.....). Results for  $t/T = \{2.9, 4.8, 8.9\}$ : — DNS; --- RANS models

### 5. Validation case: isolated vortex

Before attempting to compute the wingtip flow, the case of the temporal evolution of an isolated turbulent Batchelor vortex is investigated. The idealized axisymmetric field is fairly representative of the mean flow field of practical trailing vortices.

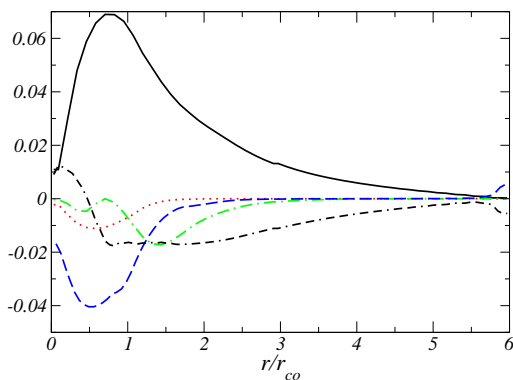


FIGURE 3. Budget of  $C_{as}$  model showing most significant contributions at  $t/T = 2.9$ , with Term numbering referring to 3.2: - - - Term 2; — Term 3; ····· Term 5; - - - Term 6; - · - · - Transport of  $C_{as}$

### 5.1. DNS of Batchelor vortex

During their work in the CTR Summer Program 2006, Drs. Duraisamy and Lele have carried out Direct Numerical Simulation (DNS) of Batchelor vortex flows. Their primary motivation was to gain a clearer understanding of the temporal evolution of vortices which are normal mode unstable (i.e. swirl number,  $q < 1.5$ ). They examine the complex evolution of helical instabilities, noting that these cases are characterised by a steep initial growth of the turbulent kinetic energy, followed by saturation and eventual decay.

The initial base flow condition for tangential velocity,  $v_\theta$  and axial velocity,  $v_x$ , is given by:

$$v_\theta = -\frac{v_o}{r\sqrt{\alpha}} \left(1 - e^{-\alpha r^2}\right), \quad v_x = -\frac{v_o}{q} e^{-\alpha r^2}, \quad (5.1)$$

where  $\alpha = 1.25643$  so that the initial vortex core-radius is  $r_{co} = 1$ . Time is non-dimensionalised by the ‘turnover time’  $T = 2\pi v_o / r_{co}$ , and the Reynolds number (defined as  $2\pi v_o / \sqrt{\alpha} \nu$ ) is set to 8250 (corresponding to  $q = 0.5$ ). They used a domain of width  $15r_{co}$  and a mesh size of  $18.87 \times 10^6$  cells.

It is beyond the ability and requirements of a turbulence model to correctly compute the complex interactions of the helical structures described by the DNS, and so the focus of this validation work is put on the decay phase of the vortex evolution. Indeed it is these same issues involved with the decay of the isolated vortex which dictate the performance of turbulence models in the wingtip vortex case, where cost constraints require the use of RANS.

### 5.2. Results

The time evolution of an isolated vortex is calculated using a 2D square grid of  $80 \times 80$  cells, with a spanwise extent of  $10r_{co}$ . Periodic boundary conditions were used in the axial flow direction and symmetry conditions were used in the directions normal to the axial flow. This is somewhat different to the conditions specified in the DNS calculations, where a more complex matching procedure was used in order to account correctly for the vanishing of the vorticity at the boundaries.

Results are displayed in figure 2 for the three RANS models: a) the SSG Reynolds

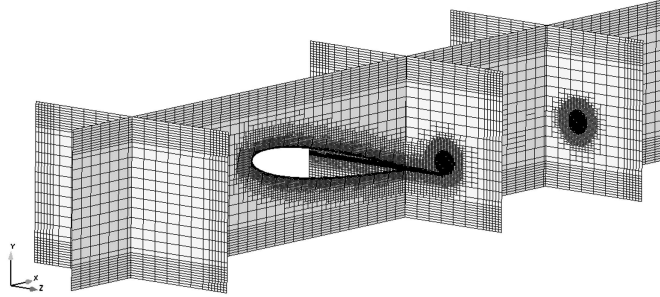


FIGURE 4. The unstructured mesh used in this work: a  $XY$  plane and two  $YZ$  planes. Total no of cells = 746,695

stress model, **b)** the standard SST model and **c)** the new SST- $C_{as}$  model. In each case the calculations were initialized using DNS data from the results for  $q = 0.5$  at  $t/T = 2.0$ , at which point the instabilities are seen to be saturated, and the mean flow is subsequently seen to revert back to equilibrium.

It is seen from figure 2a, that the Reynolds stress model appears to do a reasonable job of capturing the slow decay of both the axial and tangential velocity components. The tangential component appears to fall to zero too fast beyond  $r/r_{co} > 5$  but this is observed in the results from all three RANS models, and is most likely due to either an insufficient domain, or inadequate boundary conditions, or both. The predicted levels of  $k$  close to the vortex core are in reasonable agreement with the DNS, although there is no peak observed between  $1 < r/r_{co} < 2$ .

The predictions from the standard SST model in figure 2b are considerably worse than the RSM, with the vortex appearing to decay at a greater rate. It can also be seen to spread out more from the plots of  $U_\theta$ , which is an indicator of excessive diffusion. In corroboration with this observation, the levels of turbulent kinetic energy predicted by the SST are higher than the DNS levels, which would lead to overpredictions of both production  $P_k$  and the turbulent diffusion.

The results returned from the SST- $C_{as}$  model are broadly in agreement with the RSM predictions, and it appears that an improved modeling of  $P_k$  leads to a more accurate prediction of the levels of  $k$  and thus the mean velocities.

The budget of the transport equation for  $C_{as}$  is shown in figure 3 at  $t/T = 2.9$ , where the Term numbering refers to 3.2. Terms 1 and 4 have been omitted for clarity since they are almost zero across the vortex. The dominant Term 3 is related to the production term, and appears to be concentrated around an annulus that moves radially outward with time. Term 6 is the other dominant term, which peaks at a point closer to the core of the vortex. It is important to note that no numerical difficulties are experienced in the calculation of Term 6, which is often expected to be problematic particularly in regions where the mean velocity gradients are large.

In conclusion it appears that the SST- $C_{as}$  model should be suitable for the prediction of the mean flow in the wake of the Bradshaw wingtip, and in particular it should be able to correctly predict the decay rate of the trailing vortex.

## 6. The Bradshaw wingtip

### 6.1. Case details

The experiment of Chow *et al.* (1997) corresponds to a rounded NACA0012 wing of 4' chordlength,  $c$ , and 3' span in a wind tunnel section of 32"  $\times$  48". The chord based Reynolds number is  $4.6 \times 10^6$ , the Mach number is approximately 0.1 and the angle of attack is  $10^\circ$ . The freestream turbulent intensity is set at 0.02, and in the experiment, the flow is tripped at the leading edge so that the flow can be considered to be fully turbulent.

### 6.2. Numerical setup

The fully unstructured mesh used for the calculation in this work contains a total of just under 750,000 cells, and maintains a cross-stream mesh spacing of  $0.003c$  in the vortex core as recommended by Duraisamy & Iaccarino (2005). A perspective view of this mesh is shown in figure 4 where the cell distribution is displayed over three slices through the domain.

The mean flow was computed with two RANS models: the original SST model and the new SST- $C_{as}$  model. A fully central differencing scheme was employed for the momentum equations. It was necessary to use an upwind scheme for the start of the calculation, so as to aid convergence. A timestep of 0.001s was used to ensure that the maximum Courant number was below 1 at all times. Around 10,000 timesteps were required to obtain fully converged solutions. The additional computational expense, per timestep, of the SST- $C_{as}$  model over the SST model was 15 – 20%.

### 6.3. Results

Figures 5 and 6 display a comparison of the two RANS models with the experimental data for mean axial velocity and mean cross-flow (tangential) velocity respectively.

In figure 5a the rapid decay of the axial velocity predicted by the SST model is evident. The core value is already much lower than the experimental value by  $x = 0.24c$  downstream of the trailing edge and by  $x = 0.67c$  the axial velocity has all but disappeared off the scale shown.

Figure 5b shows the corresponding results from the SST- $C_{as}$  model and it is possible to see that there is a higher value of axial velocity at the core at  $x = 0.24c$  than with the standard SST. Despite this, the predicted peak value is noticeably less than that reported in the experiment (figure 5c). However the main difference between the two RANS models is viewed in the plots of the planes at  $x = 0.44c$  and  $x = 0.67c$ . While the SST model predicts that the vortex decays, the SST- $C_{as}$  model reproduces the axial-velocity overshoot discussed in Section 1. Lower turbulent viscosity in the vortex core region serves to reduce the production of turbulent kinetic energy and also the turbulent diffusion of momentum. This prevents a premature decay of the core axial velocity to a value well below that found in the free-stream.

Values of  $C_{as}$  in this region are close to zero and eventually reach small negative values at the vortex core. This implies a negative production term, which acts as a means of back transfer of energy from the turbulence to the mean flow.

Figure 6 reports similar findings although the improvement of the SST- $C_{as}$  over the SST is less marked. It appears that the peak cross-flow velocities are not particularly well resolved with respect to the experimental data. One explanation for this can be obtained from figure 4: it is possible that at some point along the path of the trailing vortex, the region of peak cross-flow velocity passes through a region of coarse grid cells in the

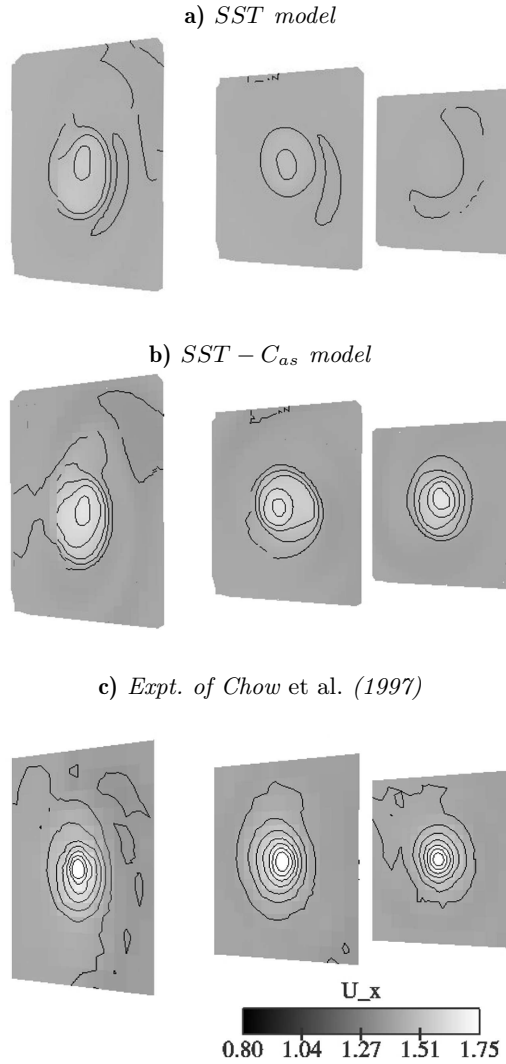


FIGURE 5. Contour plots of mean axial velocity,  $U_x$ , at three planes downstream of trailing edge: from left to right,  $x/c = \{0.24, 0.44, 0.67\}$ . Eight contours at regular intervals from 0.8 to 1.75.

unstructured mesh. In this event it is likely that a reduced peak value would be expected to be passed downstream.

It has already been noted from figures 5 and 6 that the results reported at the first plane  $x = 0.24c$  are not in perfect agreement with the experimental data. This may have more to do with mesh refinement around the wingtip itself, since in some locations the near-wall mesh is less than optimal.

## 7. Conclusion

This is ongoing work and despite a few unresolved issues, some early conclusions can be found. The use of the SST- $C_{as}$  model appears to offer some advantages over the

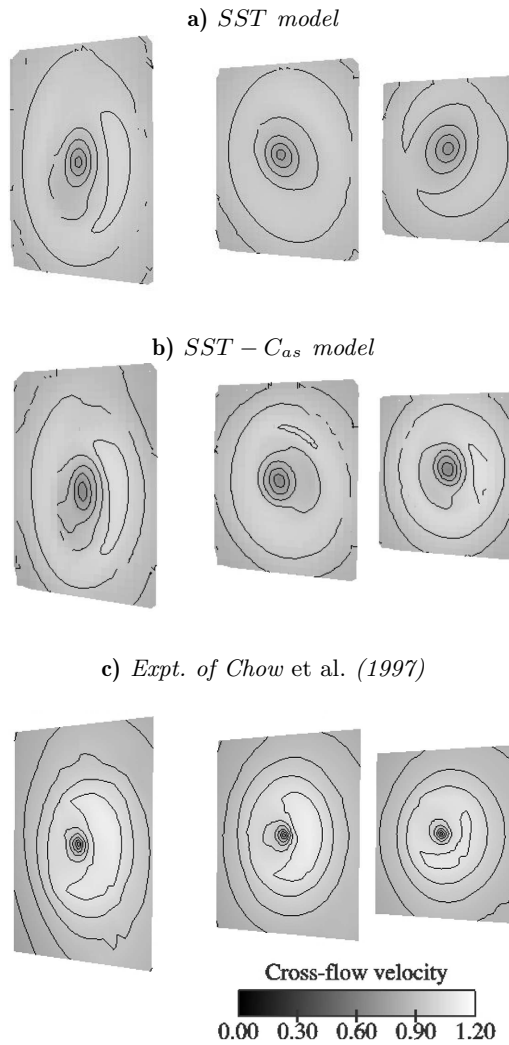


FIGURE 6. Contour plots of mean cross-flow velocity at three planes downstream of trailing edge: from left to right,  $x/c = \{0.24, 0.44, 0.67\}$ . Eight contours at regular intervals from 0.0 to 1.2.

standard SST model for the prediction of the correct decay rate of a vortex, both in the 2D validation case and the 3D case in the wake of the wingtip. The  $C_{as}$  model brings additional modelling to the SST model via the eddy viscosity, and thus the production of turbulent kinetic energy, and this appears to prevent the overprediction of  $k$  in the vortex core. The characteristic of fast decay of standard EVMs is avoided, and instead, results are seen to be similar to those found when using Reynolds stress transport models.

The modeling scheme for  $C_{as}$  presented in this work remains in its infancy and much further work would be required before an optimal form could be confidently applied to a range of flows. One such area is the issue of how to deal with  $C_{as}$  near to a solid boundary.

These are the first calculations on a fully unstructured mesh reported for this flow,

and further testing is necessary to ensure that a grid-independent solution is reached. In particular, further work will investigate mesh refinement near to the airfoil surface and around the trailing vortex itself.

## Acknowledgments

AR gratefully acknowledges support from CTR during the Summer Program 2006. AR would also like to thank Dr. K. Duraisamy for the provision of the DNS data, and Dr. T. Craft and Prof. D. Laurence for discussions about modelling issues. This work was partially supported by the DESider Project, funded by the European Community in the 6th Framework Programme, under contract No. AST3-CT-2003-502842.

## REFERENCES

- ARCHAMBEAU, F., MECHITOUA, N. & SAKIZ, M. 2004 A finite volume method for the computation of turbulent incompressible flows - industrial applications. *Int. J. Finite Volumes* **1**, 1-62.
- BALDWIN, B. S. & BARTH, T. J. 1990 A 1-equation turbulence model for high-Reynolds number wall-bounded flows. *TM 102847* NASA.
- BATCHELOR, G. K. 1964 Axial Flow in Trailing Line Vortices. *J. Fluid Mech.* **20**, 645-658.
- BERGSTROM, D. J. & WANG, B.-C. 2005 A dynamic non-linear subgrid-scale stress model. *Phys. Fluids* **17**, 3.
- CHOW, J. S., ZILLIAC, G. G. & BRADSHAW, P. 1997 Mean and turbulence measurements in the near field of a wingtip vortex. *AIAA J.* **35** 10.
- CRAFT, T. J., INCE, N. Z. & LAUNDER, B. E. 1996a Recent developments in second-moment closure for buoyancy-affected flows. *Dyn. Atmos. Oceans* **25**, 99-114.
- CRAFT, T. J., LAUNDER, B. E., & SUGA, K. 1996b Development and application of a cubic eddy-viscosity model of turbulence. *Int. J. Heat Fluid Flow* **17**, 108-115.
- CRAFT, T. J., GERASIMOV, A. V., LAUNDER, B. E. & ROBINSON, C. M. E. 2006 A computational study of the near-field generation and decay of wingtip vortices. *Int. J. Heat Fluid Flow* **27** 684-695.
- DACLES-MARIANI, J., ZILLIAC, G., CHOW, J. S. & BRADSHAW, P. 1995 Numerical/experimental study of a wingtip vortex in the near field. *AIAA J.* **33**, 1561-1568.
- DE JONG, F. J., GOVINDAN, T. R., LEVY, R. & SHAMROTH, S. J. 1988 Validation of a forward marching procedure to compute tip vortex generation processes for ship propeller blades. *Report R88-920023*, Scientific Research Associates Inc.
- DURASAMY, K. & IACCARINO, G. 2005 Curvature correction and application of the  $v^2 - f$  turbulence model to tip vortex flows. *CTR. Annual Research Briefs 2005*, Stanford.
- DURBIN, P. A. 1991 Near wall turbulence closure modeling without damping functions. *Theo. Comp. Fluid Dyna.*, **3**.
- HAASE, W., AUPOIX, B., BUNGE, U. & SCHWAMBORN, D. (EDS.) 2006 FLOMANIA - A European Initiative on Flow Physics Modelling - Results of the European-Union funded project 2002-2004. (ISBN 3-540-282786-8).
- LÜBCKE, H., RUNG, T. & THIELE, F. 2002 Prediction of the spreading mechanism of

- 3D turbulent wall jets with explicit Reynolds stress closures. *Proceedings of ETMM5*, 127-145.
- MENTER, F. R. 1994 Two equation eddy-viscosity turbulence models for engineering applications. *AIAA J.* **32**, 1598-1605.
- OLSEN, M. E. & COAKLEY, T. J. 2001 The lag model, a turbulence model for non equilibrium flows. *AIAA 2001-2564*.
- ORLOFF, K. L. 1974 Trailing Vortex Wind-Tunnel Diagnostics with a Laser Velocimeter. *J. Aircraft* **11**, 8, 477-482.
- REVELL, A. J., BENHAMADOUCHE, S., CRAFT, T. & LAURENCE, D. 2006 A stress strain lag eddy viscosity model for unsteady mean flow. *Int. J. Heat Fluid Flow* **27**, 821-830.
- REVELL, A. J. 2006 A stress - strain lag eddy viscosity model for mean unsteady turbulent flows. PhD thesis, University of Manchester.
- ROTTA, J. C. 1979 A family of turbulence models for three-dimensional thin shear layers. In Durst, F. e. a., editor, *Turbulent Shear Flows 1*, 267-278, Berlin. Springer-Verlag.
- RUNG, T. & THIELE, F. 1996 Computational modelling of complex boundary-layer flows. *Int. Symp. on Transport Phenomena in Thermal-Fluid Engineering*, 321-326.
- SPEZIALE, C. G., SARKAR, S., & GATSKI, T. B. 1991 Modeling the pressure strain correlation of turbulence: an invariant dynamical systems approach. *J. Fluid Mech.* **227**, 245-272.
- THOMPSON, D. H. 1983 A Flow Visualization Study of Tip Vortex Formation. *Aero Note 421* ARL.
- UZUN, A., HUSSAINI, M. Y. & STREETT, C. L. 2006 Large-Eddy Simulation of a wingtip vortex on overset grids. *AIAA J.* **44**, 6, 1229-1242.
- ZEMAN, O. 1995 The persistence of trailing vortices, a modeling study. *Phys. Fluids* **7**, 135-143.